Gamma-distorted fringe image modeling and accurate gamma correction for fast phase measuring profilometry

Zhongwei Li[1,2] and Youfu Li[2,*]

[1]*State Key Laboratory of Material Processing and Die & Mould Technology, Huazhong University of Science and Technology, Wuhan, China*

[2]*Department of Manufacturing Engineering and Engineering Management, City University of Hong Kong, Hong Kong, China*

**Corresponding author: meyfli@cityu.edu.hk*

Received August 30, 2010; revised October 19, 2010; accepted October 27, 2010; posted December 6, 2010 (Doc. ID 134241); published January 7, 2011

In fast phase-measuring profilometry, phase error caused by gamma distortion is the dominant error source. Previous phase-error compensation or gamma correction methods require the projector to be focused for best performance. However, in practice, as digital projectors are built with large apertures, they cannot project ideal focused fringe images. In this Letter, a thorough theoretical model of the gamma-distorted fringe image is derived from an optical perspective, and a highly accurate and easy to implement gamma correction method is presented to reduce the obstinate phase error. With the proposed method, high measuring accuracy can be achieved with the conventional three-step phase-shifting algorithm. The validity of the technique is verified by experiments.

OCIS codes: 120.2830, 120.6660, 110.6880.

Phase-measuring profilometry (PMP) has been recognized as one of the most effective methods for practical 3D phase measurements [1]. In practice, there are many factors affecting the precision of the resulting 3D measurement. These factors can be classified as being from uncertainty due to sensor noise or from a nonlinear response of gamma distortion in the camera–projector pair [2]. In contrast to measurement uncertainty that is phase independent, gamma distortion leads to the deviation of the captured fringe pattern from ideal sinusoidal waveforms and introduces an additional phase error. This kind of phase error can be eliminated by using a large number of phase-shifting fringe patterns [3]. However, in fast or real-time PMP systems [4,5], a three-step phase-shifting method is commonly used, and phase error caused by gamma distortion is considered as the dominant error source.

To overcome the gamma distortion problem, many approaches of phase-error compensation or gamma correction have been proposed [6–8]. Although most of the previous methods can reduce the phase error to a certain extent, they require the projector to be focused for best performance. However, to maximize the brightness of the projected pattern, digital projectors are usually built with large apertures in practice. The trade-off between focusing and brightness results in narrow depths of field of the projectors. Therefore, in practical PMP systems, there is only a small measurement range with sharp focus, out of which varying degrees of out-of-focus blur would occur. Although some experimental researches [9–11] indicate that rationally defocusing the projector is good for PMP systems, theoretical study about this issue is still lacking. Furthermore, a rigorous gamma distortion model and gamma calibration method that considers the defocusing effect has not yet been unveiled. In this Letter, a complete theoretical model of the gamma-distorted fringe image is derived from an optical perspective. Based on this model, a high accuracy and easy implementation gamma correction method is developed for fast PMP systems.

Mathematically, the gamma of a digital projector brings high-order harmonics to the projected fringe image, and the intensity of the gamma-distorted fringe image can be expressed as

$$I_n^P(x,y) = \{A^P(x,y) + B^P(x,y)\cos[\phi(x,y) + \delta_n]\}^\gamma = A(x,y) + \sum_{k=1}^{\infty} B_k(x,y)\cos\{k[\phi(x,y) + \delta_n]\}, \quad (1)$$

where (x,y) denotes an arbitrary point in the image, $A^P(x,y)$ and $B^P(x,y)$ are user defined constants, δ_n represents a phase-shifting amount, γ is the gamma value, $A(x,y)$ denotes the direct component, $B_k(x,y)$ denotes the magnitude of the kth harmonic component, and $\phi(x,y)$ is the desired phase information. For convenience, (x,y) will be omitted from the equations hereafter.

Following the derivation presented in [6], if $B_k \neq 0$, the ratio B_{k+1}/B_k can be derived as

$$B_{k+1}/B_k = (\gamma - k)/(\gamma + k + 1). \quad (2)$$

This is the ideal model of the gamma-distorted fringe image. As we have described before, digital projectors are built with large apertures, which prevents them from projecting ideal focused fringe images. This phenomenon can be modeled by the point spread function (PSF) of the projector. While the PSF depends on the lens system, it can be modeled as a 2D circular Gaussian of the form [12]

$$G(x,y) = \frac{1}{2\pi\sigma^2}\exp\left(-\frac{x^2+y^2}{2\sigma^2}\right), \quad (3)$$

where σ is the standard deviation of the distribution and it determines the degree of smoothing. In most practical PMP systems, as the projector is quite bright, we stop-down the aperture of the camera so that any defocus introduced by the camera is negligible compared to that of

the projector. Therefore, the actual intensity of the defocused gamma distortion fringe images can be expressed as

$$I_n^C = \alpha I_n^P * G(x,y), \tag{4}$$

where * denotes convolution and $\alpha \in [0,1]$ is the reflectivity of a scanned object. This convolution is a low-pass filter, which can suppress the high-order harmonics and accordingly reduce the phase error. To demonstrate this, the optical transfer function (OTF) of the projection optics is derived by taking the Fourier transform of the PSF. In practice, the fringe patterns are either vertical or horizontal, and because only one cross section perpendicular to the fringe patterns needs to be considered, the problem is reduced to a 1D problem and the OTF can be expressed as

$$T(f) = \int_{-\infty}^{\infty} G(x)\exp(i2\pi f x)\mathrm{d}x = \exp(-2\pi^2\sigma^2 f^2). \tag{5}$$

For sinusoidally varying the object intensity, the image intensity is equal to the object intensity multiplied by the OTF. Similarly, the captured distorted fringe can be given by

$$I_n^C = \alpha I_n^P T(f) = \tilde{A} + \sum_{k=1}^{\infty} \tilde{B}_k \cos[k(\phi + \delta_n)], \tag{6}$$

where $\tilde{A} = \alpha A$, and $\tilde{B}_k = \alpha T(kf_0)B_k$. The coefficients $T(kf_0)$ decay according to Eq. (5), providing the desired low-pass filtering effect. For any reasonable OTF, the magnitude decreases rapidly as f becomes large. Comparing Eq. (6) with Eq. (1), we can see that projector defocus will attenuate the high-order harmonics of the gamma-distorted fringe patterns.

So far, a more precise mathematical model is derived for the gamma-distorted fringe image. Consequently, we can more accurately establish the practical magnitude of the residual phase error for the three-step phase-shifting method. In this Letter, in Eq. (6), we only consider harmonics up to the third order. Nevertheless, it should be noted that the following derivation can be easily extended to higher-order harmonics and other phase-shifting methods.

Using Eq. (6) in the three-step phase-shifting method, the measured phase ϕ' can be given as

$$\phi' = -\arctan\left[\frac{\tilde{B}_1\sin(\phi) - \tilde{B}_2\sin(2\phi)}{\tilde{B}_1\cos(\phi) + \tilde{B}_2\cos(2\phi)}\right]. \tag{7}$$

The measured phase ϕ' can be considered as the sum of the actual phase ϕ and the phase error $\Delta\phi$. Thus, the phase error can be derived as

$$\Delta\phi = -\arctan\left\{\left[\frac{\tilde{B}_2}{\tilde{B}_1}\sin(3\phi)\right] / \left[1 + \frac{\tilde{B}_2}{\tilde{B}_1}\cos(3\phi)\right]\right\}. \tag{8}$$

To gauge the magnitude of the phase error, by setting $\mathrm{d}\Delta\phi/\mathrm{d}\phi = 0$, the maximum phase error of the three-step phase-shifting method can be obtained. That is,

$$\Delta\phi_{\max} = \arctan\left\{\left[\frac{(\tilde{B}_2/\tilde{B}_1)^2}{1-(\tilde{B}_2/\tilde{B}_1)^2}\right]^{1/2}\right\} = \arctan\left[\left(\frac{p^2}{1-p^2}\right)^{1/2}\right], \tag{9}$$

where

$$p = \frac{\tilde{B}_2}{\tilde{B}_1} = \frac{T(2f_0)}{T(f_0)}\frac{B_2}{B_1} = \exp(-6\pi^2\sigma^2 f_0^2)\frac{\gamma-1}{\gamma+2}. \tag{10}$$

Through the equations above, we can know that the phase error is not only related to gamma value (γ), phase steps (N), and phase value (ϕ), but it is also related to the defocus degree (σ) and spatial carrier frequency (f_0). The maximal phase error monotonically increases in the scope of $p \in (0,1)$, and as $T(2f_0)/T(f_0) < 1$, the defocus decreases the ratio p and accordingly reduces the maximal phase error. This is the theoretical cause of why proper projector defocus is good for weakening the effects of gamma distortion. Nevertheless, at the same time, the defocusing effect will make the phase error unsteady and variational in the measuring space. One feasible way to solve this problem is gamma correction, which calibrates the accurate gamma value and encodes it to the generated phase-shifting images. In this Letter, based on the derived mathematical model, an accurate gamma correction method is developed.

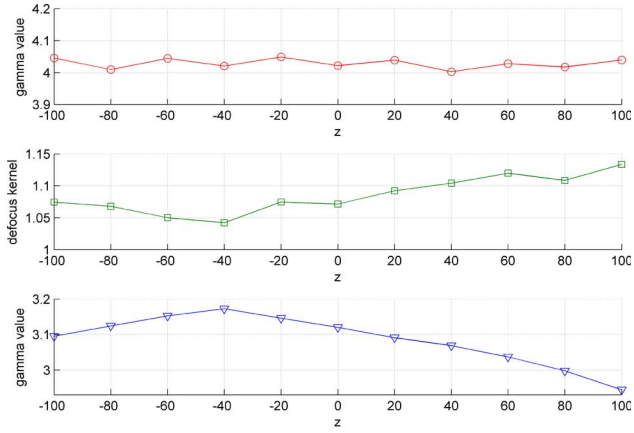

(a)

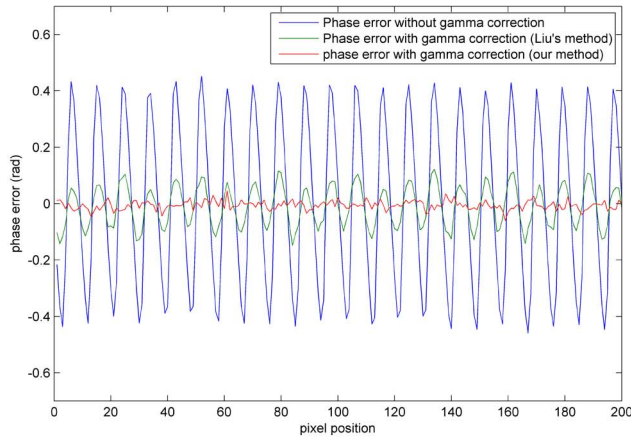

(b)

Fig. 1. (Color online) Experiment results: (a) gamma calibration results and (b) phase errors without and with gamma correction.

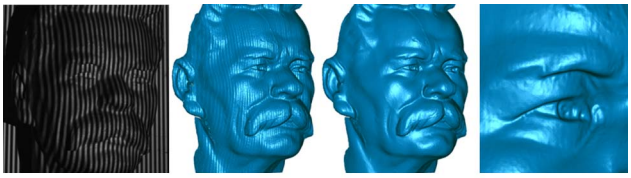

(a) (b) (c) (d)

Fig. 2. (Color online) Measurement result of a complex plaster model: (a) captured fringe image, measured 3D surface (b) without and (c) with our gamma correction, and (d) partial enlarged detail.

According to discrete-time Fourier series, $\tilde{B}_1$ and $\tilde{B}_2$ can be expressed as

$$\tilde{B}_k = \frac{1}{L}\left\{\left[\sum_{l=1}^{L} I_l^C \sin\left(k\frac{2\pi l}{L}\right)\right]^2 + \left[\sum_{l=1}^{L} I_l^C \cos\left(k\frac{2\pi l}{L}\right)\right]^2\right\}^{1/2}, \tag{11}$$

where $k = 1, 2$, and L is the number of patterns. The effect of the high-order harmonic on the main harmonic depends on the number of patterns L; the larger is L, the smaller is the effect of the high-order harmonic. Therefore, we can estimate correct $B_2/\tilde{B}_1$ from Eq. (11) with a large L. We note that Eq. (11) is consistent with the equation derived by [6]. However, they do not consider the influence of the projector defocusing effect and directly take $\tilde{B}_2/\tilde{B}_1$ for B_2/B_1 to calculate γ from Eq. (2). Actually, $\tilde{B}_2/\tilde{B}_1$ is less than B_2/B_1 owing to the influence of the defocusing, so γ calculated from their method is less than the actual one.

From Eqs. (10) and (11), we can know that, with an arbitrary none-1 encoding γ' preapplied to the computer-generated fringe images, the ratio $\tilde{B}_2'/\tilde{B}_1'$ can be expressed as

$$\frac{\tilde{B}_2'}{\tilde{B}_1'} = \frac{T(2f_0)}{T(f_0)}\frac{B_2'}{B_1'} = \exp(-6\pi^2\sigma^2 f_0^2)\frac{\gamma/\gamma' - 1}{\gamma/\gamma' + 2}. \tag{12}$$

Similarly, we can also estimate correct $\tilde{B}_2'/\tilde{B}_1'$ from Eq. (11) with a large L. Then, combining Eqs. (10) and (12), we can easily calculate γ and σ for each pixel. In practice, γ at each pixel is not exactly the same. So a trade-off solution is to apply a mean gamma value $\bar{\gamma}$ to encode the computer-generated phase-shifting images.

The above approach is summarized as:

1. With a simple-shape object (e.g., a white flat board) as a target, we use two groups of phase-shifting fringe images with a large L (e.g., $L = 16$), encoded with $\gamma' = 1$ and $\gamma' = 2$, to calculate $\tilde{B}_2/\tilde{B}_1$ and $\tilde{B}_2'/\tilde{B}_1'$, respectively, according to Eq. (11).
2. Calculate γ and σ for each pixel according to Eqs. (10) and (12), and estimate the mean gamma value $\bar{\gamma}$. Then, encode $\bar{\gamma}$ to the computer-generated three-step phase-shifting images.
3. Once $\bar{\gamma}$ is calibrated and encoded to the generated phase-shifting images, a conventional three-step phase-shifting method can be used to retrieve phase with gamma distortion removed.

The performance of the proposed gamma correction method was verified with a PMP system composed of a digital projector (Infocus LP70+) and a CCD camera (DH-1410FM). A white flat board was put in front of the system, perpendicular to the optical axis of the projector. The projected images were adjusted to be in focus on the board manually. Then, applying the proposed method, a gamma matrix with a reliably estimated mean gamma value $\bar{\gamma}$ can be calculated. For comparison, the Liu method [6] was also employed to obtain the $\bar{\gamma}$. Then we moved the flat board to ten different positions before and after the focus plane, with an interval of 20 mm, and we repeated the above process. The obtained $\bar{\gamma}$ are shown in Fig. 1(a). From the top and bottom figures, we can see that $\bar{\gamma}$ obtained from our method vary in a small range (from 4.01 to 4.05), while the ones obtained from the Liu method have smaller values but with a bigger range of change (from 2.95 to 3.17). The obtained σ are plotted in the middle figure. It is seen that, at $z = -40$ mm, σ is minimum, being equal to 0.92. Accordingly, the $\bar{\gamma}$ obtained from the Liu method is maximum. It is because at this position, the projected image is at optimal focus. Therefore, the effect of defocusing is the minimum. These results agree well with the theoretical model. The phase errors obtained from the three-step phase-shifting method without and with gamma correction are shown in Fig. 1(b). The actual phase values are obtained from a 16-step phase-shifting method. The maximal phase error before gamma correction is 0.464 rad. Preencoding the gamma value obtained from Liu's method and our method, the maximal phase error reduces to 0.137 and 0.045 rad, respectively. The results show that our method is more accurate.

Next, a plaster model with free-form surface is measured with our gamma correction method. The measurement result is given in Fig. 2. The measured 3D surface with our gamma correction method shows that there is no obvious ripple on the 3D surface, which indicates that our gamma correction method can significantly improve the measuring precision.

The work was supported by the Research Grants Council of Hong Kong (CityU117507), the China Postdoctoral Science Foundation (20090460944), and the National Natural Science Foundation of China (NSFC) (51005090).

References

1. S. Gorthi and P. Rastogi, Opt. Lasers Eng. **48**, 133 (2010).
2. Z. Wang, D. Nguyen, and J. Barnes, Opt. Lasers Eng. **48**, 218 (2010).
3. T. Hoang, B. Pan, D. Nguyen, and Z. Wang, Opt. Lett. **35**, 1992 (2010).
4. K. Liu, Y. Wang, D. Lau, Q. Hao, and L. Hassebrook, Opt. Express **18**, 5229 (2010).
5. S. Zhang, Opt. Lasers Eng. **48**, 149 (2010).
6. K. Liu, Y. Wang, D. Lau, Q. Hao, and L. Hassebrook, J. Opt. Soc. Am. A **27**, 553 (2010).
7. B. Pan, K. Qian, L. Huang, and A. Asundi, Opt. Lett. **34**, 416 (2009).
8. S. Zhang, S. T. Yau, Appl. Opt. **46**, 36 (2007).
9. X. Su, W. Zhou, and G. Bally, Opt. Commun. **94**, 561 (1992).
10. C. Coggrave and J. Huntley, Opt. Eng. **39**, 91 (2000).
11. S. Lei and S. Zhang, Opt. Lett. **34**, 3080 (2009).
12. M. Brown, P. Song, and T. Cham, in *Proceedings of the 2006 IEEE Computer Society Conference on Computer Vision and Pattern Recognition* (IEEE, 2006), p. 1956.